

Residual stresses in polycrystalline sheet silicon and it's relation to lifetime

S. He, S. Danyluk*

The George W. Woodruff School of Mechanical Engineering, Georgia Institute of Technology

I. Tarasov, S. Ostapenko

Center for Microelectronics Research, University of South Florida

(Dated: March 11, 2005)

This letter summarizes the research on the characterization of residual stresses and lifetime of polycrystalline sheet silicon for photovoltaic application. Full-field polariscopy, scanning room temperature photoluminescence (PL) and surface photovoltage (SPV) are used to characterize unprocessed silicon sheet. An orientation dependent stress-optic coefficient has been developed and used to extract the in-plane residual stresses. The characteristics of the spatial distribution and the quantitative correlation between the residual stresses and the lifetime is presented.

PACS numbers:

Silicon ribbon produced by edge-defined film-fed growth (EFG) or string ribbon sheet growth methods are potential materials for low cost solar cells, however, stress is one of the key issues in the crystal growth and subsequent cell processing and handling. Stresses are believed to result from crystal growth and to be roughly proportional to the curvature of the temperature profile [1, 2]. To sustain high growth speed, a large interface temperature gradient is required and the stresses generated can lead to the breakage of a typical ribbon [3, 4]. Stresses that are associated with plasticity cannot be removed completely by post-growth annealing [3]. When the ribbon is cut into blanks, the non-evenly distributed residual stress may create buckles and ripples, which makes it useless for cell fabrication [5, 6]. Furthermore, the micro-cracks in the perimeter of the wafer, and in some cases the front and back surfaces, will eventually propagate and fracture the cell in handling during subsequent device fabrication [7], if they fall in the region of tensile residual stresses.

Besides fracture, residual stresses can also generate and propagate dislocations and it is believed that this will eventually impact the lifetime and thus the efficiency of photovoltaic cells. As sheet becomes thinner, the grown-in residual stresses, coupled with the stresses imposed during manufacturing, presents a formidable challenge.

Seidensticker [7] measured the residual stresses in ribbons by splitting the crystals lengthwise and measuring the split divergence as a function of length. The residual stresses can be extracted from the divergence under certain assumption. There has been a good deal of effort devoted to the use of non-destructive methods [8–11] in measurement of residual stresses. Our research has involved the use of a full-field near infrared (NIR) circular polariscopy [12] capable of whole field mapping in a relatively short time (≤ 30 sec). The details of the setup and principles are given in other papers [13, 14]. The sen-

sitivity of the system is 1.5 MPa [15], and the spatial resolution is approximately 200 μm . In the course of our work, we have addressed a number of fundamental issues in the transmission of light through anisotropic materials. One example is the determination of the stress-optic coefficient and it's dependence on crystallographic orientation. The photoelastic parameters (δ, θ) measured by the polariscopy can be converted to stress using an orientation dependent anisotropic stress-optic law [16].

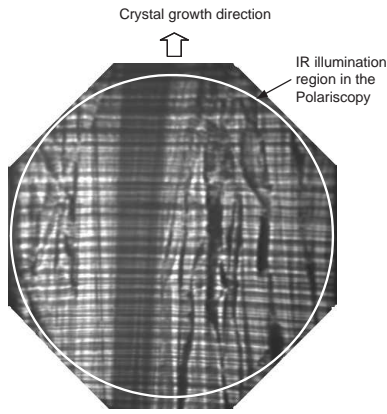
$$C(\theta) = \frac{n_0^3}{2} \frac{1}{\sqrt{\frac{\sin^2 2\theta}{\pi_{44}^2} + \frac{\cos^2 2\theta}{(\pi_{11} - \pi_{12})^2}}} \quad (1)$$

where $C(\theta)$ is the stress-optic coefficient of that depends on the crystallographic orientation of the silicon. θ is the orientation of the residual stress. π_{11}, π_{12} and π_{44} are components in the piezo-optical tensor. n_0 is the refractive index of silicon when stress free.

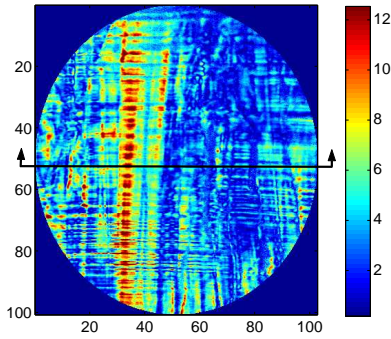
The electron-hole lifetime is another parameter that is related to cell efficiency and it is believed to be linked to the orientation dependent residual stresses. We have obtained lifetime by use of room temperature photoluminescence (PL) [17] and this paper shows the correlation between PL and the residual stresses for a grain structure orientated principally around [001]. The excitation source of the room temperature PL is an InGaAr infrared diode with a wavelength of 810 nm and power up to 55 nW, which is modulated by a mechanical chopper. Full field mapping is accomplished by using an X-Y translation stage. The spatial resolution is adjustable between 60 μm and 1 mm. Previous research [17] has shown that the results of photoluminescence are proportional to the effective lifetime, which is a combination of bulk lifetime and surface recombination velocity. The bulk lifetime was further measured by the surface photovoltage (SPV) technique with a spatial resolution of 5 mm.

Fig. 1 shows an optical image and a typical residual stress distribution in an EFG ribbon sample. The size of the sample is 80 \times 100 mm. The maximum stress is 11 MPa and the average stress is 3.28 MPa. The pattern of the residual stress is closely related to that of

*Electronic address: steven.danyluk@marc.gatech.edu



(a) Photograph of an EFG wafer, indicating the growth direction and region of IR illumination.



(b) Residual stress distribution in the illuminated region, a scan through the central region as shown in this figure is shown in FIG. 2

FIG. 1: Residual stress in an EFG wafer

the crystal structure with strips of high stress following the crystal growth direction. Strong spatial variation and stress concentration are also observed in the distribution.

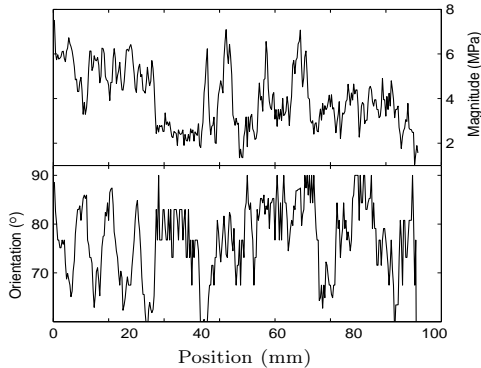


FIG. 2: Magnitude and orientation of the residual stress at an arbitrary section perpendicular to the growth direction

Fig. 2 shows the stress distribution of an arbitrary cross section perpendicular to the growth direction. The

main reason for the spatial variation is the relatively small grains and relatively large number of grain boundaries. The orientation of the residual stresses is critical to the propagation of micro cracks because it determines the crack propagation mode. The fracture toughness, K_{Ic} , is lower for mode I, or opening mode crack [18]. Fig. 2 also shows the orientation of the residual stress. It can be seen that the orientation of the residual stress falls into a narrow range from 70° to 90° , which is close to the crystal growth direction.

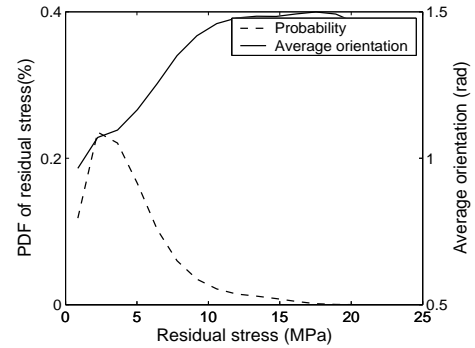


FIG. 3: Probability distribution of the magnitude of residual stress in a silicon ribbon

Fig. 3 shows the probability density function (PDF) of the magnitude of the residual stress. The shape of the PDF is close to an χ^2 distribution. The solid line in the figure shows the average orientation for the areas with the same magnitude of stress. This curve shows that as the magnitude of the residual stresses increases, the average orientation is closer to 90° , which means that the stress with a high magnitude is more likely aligned along the crystal growth direction.

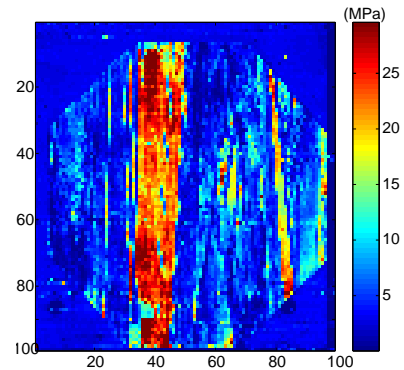


FIG. 4: PL of the EFG wafer

Fig. 5 shows the typical photoluminescence and surface photovoltage (SPV) of the same silicon ribbon. The SPV pattern is similar to that of the residual stress with strips along the crystal growth direction. A spatial correlation between the residual stresses, photoluminescence

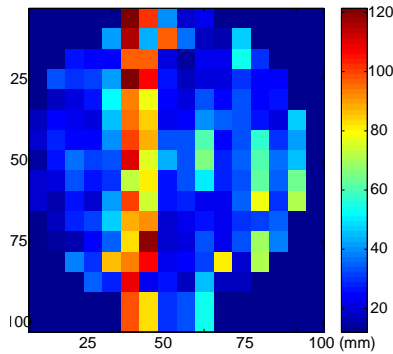


FIG. 5: SPV of the EFG wafer

and SPV can be observed when comparing these two mappings with the residual stress shown in Fig. 1. The high residual stress areas are correlated to the high PL and SPV, or high lifetime areas. The reason for this correlation is that in the high residual stress areas, the residual stresses are locked-in; therefore fewer defects are produced which act as recombination centers and thus has less impact on the minority carrier lifetime. In this sense high residual stresses are beneficial to PV efficiency.

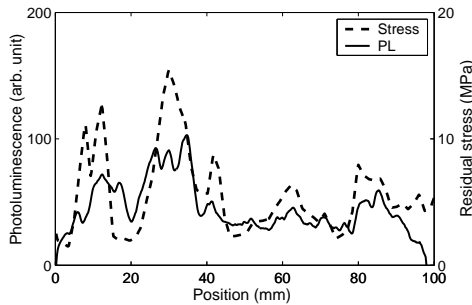


FIG. 6: Correlation between average residual stress and PL

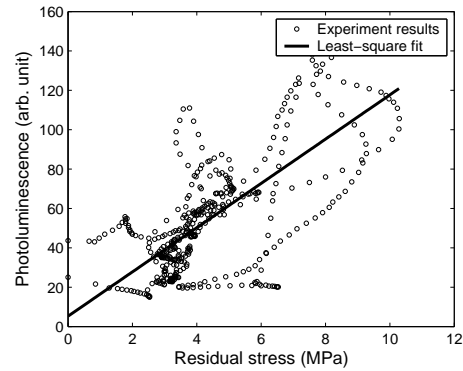


FIG. 7: Correlation between average residual stress and PL

Since both the residual stresses and photoluminescence are relatively uniform along the crystal growth direction, the average along this direction can be illustrative to demonstrate their correlation quantitatively. Fig. 6 shows the average residual stress and photoluminescence along the growth direction. It can be observed that the two curves have the same trend and the locations of peaks are closely matched. The quantitative correlation can be obtained by comparing the residual stress and the photoluminescence point-by-point. Fig. 7 shows this correlation by taking residual stress and photoluminescence as the two axes. The solid line shows the least square fit of the data. The correlation coefficient of this fit is moderate, 0.6, but a linear tendency between the residual stress and PL is clearly observed.

This project is supported by NREL under contract #AAT 2-3165-06. The authors would like to thank RWE-Schott (J. Kalejs) for providing the wafers.

-
- [1] B. Chalmers, *J. Cryst. Growth* **70**, 3 (1984).
 - [2] R. L. Wallace, J. I. Hanoka, A. Rohatgi, and G. Crotty, *Sol. Energy Mater.* **48**, 179 (1997).
 - [3] J. P. Kalejs, *J. Cryst. Growth* **230**, 10 (2001).
 - [4] C. H. Wu and J. C. Lambropoulos, *J. Cryst. Growth* **155**, 38 (1995).
 - [5] J. P. Kalejs, B. H. Mackintosh, and T. Surek, *J. Cryst. Growth* **50**, 175 (1980).
 - [6] J. C. Lambropoulos, J. W. Hutchinson, R. O. Bell, B. Chalmers, and J. P. Kalejs, *J. Cryst. Growth* **65**, 324 (1983).
 - [7] R. G. Seidensticker and R. H. Hopkins, *J. Cryst. Growth* **50**, 221 (1980).
 - [8] W. J. Bond and J. Andrus, *Phys. Rev.* **101**, 1211 (1956).
 - [9] A. T. Andonian and S. Danyluk, *J. Mater. Sci.* **20**, 4459 (1985).
 - [10] A. K. Dutta and P. K. Ajmera, *J. Appl. Phys.* **69**, 7411 (1991).
 - [11] M. Fukuzawa and M. Yamada, *J. Cryst. Growth* **229**, 22 (2001).
 - [12] E. A. Patterson, *Strain* **24**, 15 (1988).
 - [13] T. Zheng and S. Danyluk, *Materials Evaluation* **59**, 1227 (2001).
 - [14] T. Zheng and S. Danyluk, *J. Mater. Res* **17**, 36 (2002).
 - [15] S. He, T. Zheng, and S. Danyluk, in *13th Workshop on Crystalline Silicon Solar Cell Materials and Processes* (Vail Colorado, 2003).
 - [16] S. He, T. Zheng, and S. Danyluk, *J. Appl. Phys.* **x** (2004).
 - [17] S. Ostapenko, I. Tarasov, J. P. Kalejs, and C. H. E.-U. Reiser, *Semicond. Sci. Technol.* **15**, 840 (2000).
 - [18] N. E. Dowling, *Mechanical behavior of materials* (Prentice Hall, 1998).